

Stability Analysis of Backstepping Controller on Electrohydraulic System Using Disturbance Observer Mechanism

C O Ngene¹, I I Eneh²

¹Student, Department of Electrical Electronic Engineering, Enugu State University of Science and Technology Enugu, Nigeria.

²Prpofessor, Department of Electrical Electronic Engineering, Enugu State University of Science and Technology Enugu, Nigeria.

Corresponding Author: chibuokemchukwuemeka@gmail.com

Abstract: In this research, the stability analysis of a backstepping controller on electro-hydraulic system using disturbance observer mechanism is presented. The proposed controller employs the parameter adaptation law designed according to Lyapunov analysis to guarantee the stability of the close loop system and the boundedness of the parameters, which is supported by the theorem. The materials used for this research include, Data from Electro hydraulic system, Matlab software and Computer system. The hydraulic system was built using Sim Hydraulic blocks imported from Matlab and the responses were analyzed from Matlab graph. The piston position was directly proportional to the Pump pressure where the hydraulic and spring forces were balanced. Discontinuities in the velocity at 0.04 sec and 0.05 sec indicates negligible mass of the piston. The model reaches a steady state when all the pump flow goes to leakage, this results to pressure drop across the control valves and brings about equal pressure at different locations of the valves. From the analysis, the position of the piston due to leakages was relatively poor. On implementation of disturbance observer the position tracking performance of the electro-hydraulic system was improved. The research concludes that the backstepping control using disturbance observer mechanism technique provided robust performance in the operation of electro-hydraulic system.

Key Words: - Lyapunov, Pump pressure, Backstepping, Observer, Electro-hydraulic.

I. INTRODUCTION

Hydraulic actuators are used in applications that require fast motion and large actuation forces. Typical areas of application include industrial robots, material handling machines, active suspensions, motion simulators, and injection moulding machines. Indeed, hydraulic actuators are often the only viable alternative for these applications, because other actuators, such as electric motors, usually lack the necessary power, size, and speed.

Despite this extensive application, actively-controlled hydraulic systems do not fully realize their potential due to, among other factors, difficulties in modelling and controlling their highly nonlinear characteristics.

Among these components, flow control valves are the most important because they most directly affect the dynamic properties of the system. Typical flow control valves include servo valves or proportional valves (Eriksson, 2013).

The proportional and servo valves are used to regulate the oil flow rates, and thereby the motion of a hydraulic system. Due to the nature of orifice flow inside the valve body, these valves are the major source of nonlinearities in hydraulic systems. The nonlinear flow property is present regardless how precise the valve body and the enclosed spool are produced (Gamble *et al.*, 2019). In addition, most valves exhibit further nonlinearities such as deadzone due to valve spool overlap, hysteresis due to magnetic properties of the solenoid coil driver, friction, and nonlinear flow forces.

Manuscript revised April 03, 2023; accepted April 04, 2023. Date of publication April 08, 2023.

This paper available online at www.ijprse.com

ISSN (Online): 2582-7898; SJIF: 5.59

Without the proper analysis and design tools, the benefits of hydraulic systems may be overshadowed by the problems in dealing with such complex nonlinear systems (Park, *et al.*, 2016).

Most hydraulic component models have been developed for subsequent application of linear control design tools; they are therefore simple and linear. In precision motion control applications, however, the various nonlinearities mentioned cannot be ignored because they can greatly degrade the system performance (Dachee *et al.*, 2019).

Furthermore, linear control theory cannot adequately cope with nonlinearities such as deadzone or friction. Hence for such applications, linear controllers are simply not capable of providing high performance. This is especially true when economic considerations drive the use of less expensive and less precise components.

In order to fully realize the capabilities of hydraulic systems, more complete models of hydraulic systems components must be developed, and these models must be incorporated into the design of advanced controllers, (Tony, *et al.*, 2019). However, because previous observers have used the derivative of the measurement signal, which contains measurement noise, the system can become unstable due to the amplification of the noise.

To circumvent around this problem, a robust adaptive observer that can estimate states is required. Subsequently, the estimated states from the observer can be used to compute the control signal (Sohl, *et al.*, 2019).

In this work, an enhanced Lyapunov approach to disturbance observer mechanism in the stability analysis of the Backstepping controller of an electro-hydraulic system is presented.

II. MATERIALS AND METHOD

Materials:

The materials used for this work are data from electrohydraulic system, Matlab software, and related literatures.

Method:

The backstepping controller is designed to compensate for an unknown disturbance and track the desired output y_d . In this stage, nominal system parameters are used to design the observers and the controller. The proposed control system is demonstrated in Figure 1.

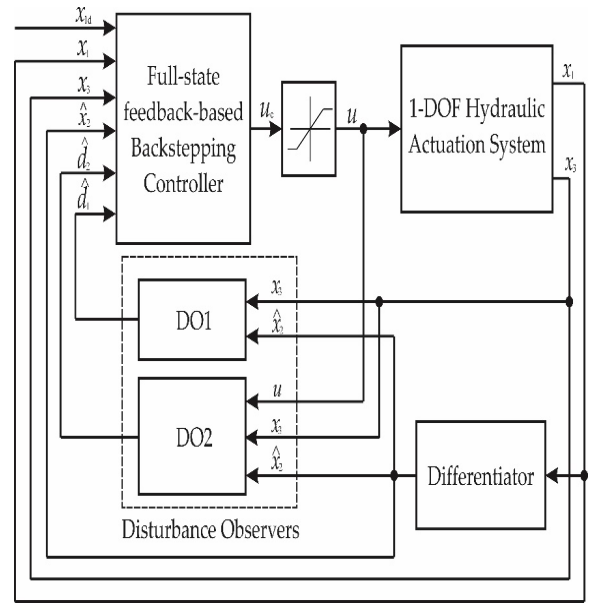


Fig.1. The proposed control system based on disturbance observers with backstepping control.

In this control system, the state observer based on the Levant's differentiator is designed to accurately approximate the angular velocity of the inertial load. The output of this observer is fed back to the controller and two disturbance observers as well. The disturbance observers are constructed to estimate the lumped uncertainties, and then they are integrated in the control design step to compensate for their effects on the closed loop control system. The controller is synthesized by using the backstepping method, which utilizes the measured states (the angular position and the pressures of chambers of the actuator), estimated state (angular velocity) produced by state observer, and the estimation of unmodeled uncertainties are generated by the disturbance observers. This control algorithm guarantees globally bounded tracking performance in the presence of the modelling error and un-modelled uncertainties.

We define the position/output tracking error z_1 as

$$z_1 = x_1 - y_d. \quad (1)$$

The states of the closed-loop system z_{cl} are defined as

$$z_{cl} = [z_1, z_2, z_3, \tilde{d}]^T \quad (2)$$

Where z_2 and z_3 are defined below:

Suppose that the control law is given by

$$z_1 = x_1 - y_d, \quad (3)$$

$$\alpha_1 = -k_1 z_1, \quad (4)$$

$$z_2 = x_2 - \dot{y}_d - \alpha_1, \quad (5)$$

$$\alpha_2 = \frac{kx_1 + bx_2 - (A_p - m)\dot{y}_d + m(-k_2 z_2 + \dot{\alpha}_1 - z_1) + \tilde{d}}{A_p}, \quad (6)$$

$$z_3 = x_3 - \dot{y}_d - \ddot{y}_d - \alpha_2, \quad (7)$$

$$u = \frac{\varphi(x,z,y_d)}{\frac{4\beta_e C_d^{wk_v}}{V_t \sqrt{\rho}} \sqrt{(P_s - \text{sgn}(\varphi(x,z,y_d)))x_3}} \quad (8)$$

Where k_1, k_2 , and k_3 are positive gains, and

$$\varphi(x, z, y_d) = \frac{4\beta_e A_p}{V_t} x_2 + \frac{4\beta_e C_{tl}}{V_t} x_3 + \ddot{y}_d + \dot{\alpha}_2 - k_3 z_3 - \frac{A_p}{m} z_2. \quad (9)$$

If we take $\frac{1}{l_0} < 4m^2 k_2$, then $z_{tl}(t)$ is globally uniformly bounded.

Proof:

The derivative of z_1 with respect to time gives us

$$\dot{z}_1 = \dot{x}_1 - \dot{y}_d = x_2 - \dot{y}_d. \quad (10)$$

Let us define the control Lyapunov function (CLF) candidate, V_1 as,

$$V_1 = \frac{1}{2} z_1^2 \quad (11)$$

The derivative of V_1 with respect to time is given by

$$\dot{V}_1 = z_1 \dot{z}_1 = z_1 (z_2 + \alpha_1) \quad (12)$$

Substituting α_1 in (8) into (12) results in

$$\dot{V}_1 = -k_1 z_1^2 + z_1 z_2 \quad (13)$$

The derivative of z_2 with respect to time gives us

$$\dot{z}_2 = \dot{x}_2 - \dot{y}_d - \dot{\alpha}_1 = -\frac{1}{m} (kx_1 + bx_2) + \frac{A_p}{m} x_3 - \frac{d}{m} - \dot{y}_d - \dot{\alpha}_1 \quad (14)$$

Let us define V_2 as

$$V_2 = V_1 + \frac{1}{2} z_1^2 + \frac{1}{2} \tilde{d}^2 \quad (15)$$

Then

$$\begin{aligned} \dot{V}_2 &= \dot{V}_1 + z_2 \dot{z}_2 + \tilde{d} \dot{\tilde{d}} \\ &= \dot{V}_1 + z_2 \left(-\frac{1}{m} (kx_1 + bx_2) + \frac{A_p}{m} x_3 - \frac{d}{m} - \dot{y}_d - \dot{\alpha}_1 \right) + \tilde{d} \dot{\tilde{d}} \end{aligned} \quad (16)$$

Substituting (7) and (8) into (16) results in

$$\dot{V}_2 = \dot{V}_1 + z_2 \left(-\frac{1}{m} (kx_1 + bx_2) + \frac{A_p}{m} (z_3 + \ddot{y}_d + \alpha_2) - \frac{d}{m} - \dot{y}_d - \dot{\alpha}_1 \right) + \tilde{d} (\dot{d} - l_0 \tilde{d}) \quad (17)$$

With α_2 , the time derivatives of V_2 becomes

$$\begin{aligned} \dot{V}_2 &= -k_1 z_1^2 + k_2 z_2^2 - \frac{1}{m} z_2 \tilde{d} + \tilde{d} (\dot{d} - l_0 \tilde{d}) + \frac{A_p}{m} z_2 z_3 \leq \\ &= -k_1 z_1^2 - k_2 \left(z_2^2 + \frac{1}{k_2 m} z_2 \tilde{d} \right) - l_0 \tilde{d}^2 + |\tilde{d}| |\dot{d}| + \frac{A_p}{m} z_2 z_3 = \\ &= -k_1 z_1^2 - k_2 \left(z_2 + \frac{1}{2mk_2} \tilde{d} \right)^2 - \gamma \left(|\tilde{d}| - \frac{1}{2\gamma} |\dot{d}| \right)^2 + \frac{1}{4\gamma} |\dot{d}|^2 + \\ &= \frac{A_p}{m} z_2 z_3 \end{aligned} \quad (18)$$

$$\text{Where } \gamma = \frac{4m^2 l_0 k_2 - 1}{4m^2 k_2}.$$

From Assumption 1, because $|\dot{d}| \leq \dot{d}_{max}$, \dot{V}_2 becomes

$$\begin{aligned} \dot{V}_2 &\leq -k_1 z_1^2 - k_2 \left(z_2 + \frac{1}{2mk_2} \tilde{d} \right)^2 - \gamma \left(|\tilde{d}| - \frac{1}{2\gamma} |\dot{d}| \right)^2 + \\ &= \frac{1}{4\gamma} |\dot{d}|^2 + \frac{A_p}{m} z_2 z_3 \end{aligned} \quad (19)$$

The dynamics of z_3 is

$$\dot{z}_3 = \frac{4\beta_e A_p}{V_t} x_2 + \frac{4\beta_e C_{tl}}{V_t} x_3 + \frac{4\beta_e C_d^{wk_v}}{V_t \sqrt{\rho}} \sqrt{(P_s - \text{sgn}(u)x_3 u - \ddot{y}_d - \dot{\alpha}_2)} \quad (20)$$

We define the overall Lyapunov function candidate V_3 as

$$V_3 = V_2 + \frac{1}{2} z_3^2 \quad (21)$$

Then we obtain \dot{V}_3 as

$$\dot{V}_3 = \dot{V}_2 + z_3 \dot{z}_3 \quad (22)$$

Substituting (20) into (22) yields

$$\begin{aligned} \dot{V}_3 &= \dot{V}_2 + z_3 \left(\frac{4\beta_e A_p}{V_t} x_2 + \frac{4\beta_e C_{tl}}{V_t} x_3 + \right. \\ &\left. \frac{4\beta_e C_d^{wk_v}}{V_t \sqrt{\rho}} \sqrt{(P_s - \text{sgn}(u)x_3 u - \ddot{y}_d - \dot{\alpha}_2)} \right) \end{aligned} \quad (23)$$

With the control input, \dot{V}_3 can be written as

$$\begin{aligned} \dot{V}_3 &= \dot{V}_2 - k_3 z_3^2 - \frac{A_p}{m} z_2 z_3 \\ &\leq -k_1 z_1^2 - k_2 \left(z_2 + \frac{1}{2mk_2} \tilde{d} \right)^2 \\ &\quad - \gamma \left(|\tilde{d}| - \frac{1}{2\gamma} \dot{d}_{max} \right)^2 - k_3 z_3^2 - \frac{1}{4\gamma} |\dot{d}|^2 \\ &\leq -(1 - \theta) \tilde{V}_{3_0} - \theta \tilde{V}_{3_0} + \frac{1}{4\gamma} \dot{d}_{max}^2 \end{aligned}$$

Where $\tilde{V}_{3_0} = k_1 z_1^2 + k_2 \left(z_2 + \frac{1}{2mk_2} \tilde{d} \right)^2 + \gamma \left(|\tilde{d}| - \frac{1}{2\gamma} \dot{d}_{max} \right)^2 + k_3 z_3^2$

and $0 < \theta < 1$. If we take $\frac{1}{l_0} < 4m^2 k_2$ and $\|z_{cl}(t)\| \geq B_r$

where $B_r = \left\{ z_{cl} \mid \theta \tilde{V}_{3_0} = \frac{1}{4\gamma} \dot{d}_{max}^2 \right\}$, then

$$\dot{V}_3 \leq -(1 - \theta) \tilde{V}_{3_0}. \quad (24)$$

Thus $z_{cl}(t)$ globally uniformly bounded.

In this work, the system, disturbance observer, and controller parameters used are as follows: $m=10$, $k=50$, $b=1000$, $A_p = 4.812 \times 10^{-4}$, $\beta_e = 1.8 \times 10^9$, $V_t = 6.2 \times 10^{-5}$, $C_{il} = 2.48815 \times 10^{-14}$, $C_{el} = 1.66 \times 10^{-14}$, $w = 5.2 \times 10^{-3}$, $\rho =$

840, $C_d = 0.6$, $k_v = 1.33 \times 10^{-5}$, $P_s = 12.0 \times 10^6$, $k_1 = 350$, $k_2 = 1700$, $k_3 = 130$, $l_0 = 1,49 \times 10^3$

Figure 2 shows the top level diagram of the model. The pump flow and the control valve orifice area are simulation inputs. The model is organized as two subsystems: the 'Pump' and the 'Valve/Cylinder/Piston/Spring Assembly'

The pump model computes the supply pressure as a function of the pump flow and the load (output) flow (Figure 3). Q_{pump} is the pump flow data. A matrix with column vectors of time points and the corresponding flow rates $[T, Q]$ specifies the flow data. The model calculates pressure p_1 as indicated in Equation Block 1. Because $Q_{out} = q_{12}$ is a direct function of p_1 (via the control valve), an algebraic loop is formed. An estimate of the initial value, p_{10} , enables a more efficient solution

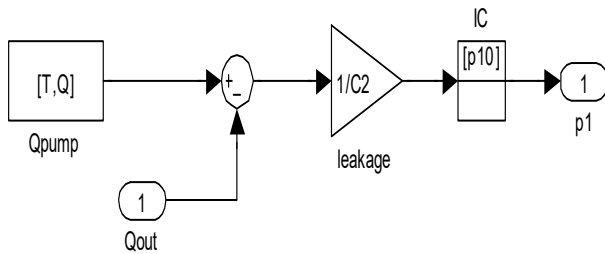


Fig.2. The pump subsystem

The Actuator subsystem, a system of differential-algebraic equations models the cylinder pressurization with the pressure p_3 , which appears as a derivative in Equation Block 3 and is used as the state (integrator). If we neglect piston mass, the spring force and piston position are direct multiples of p_3 and the velocity is a direct multiple of p_3 's time derivative. This latter relationship forms an algebraic loop around the 'Beta' Gain block. The intermediate pressure p_2 is the sum of p_3 and the pressure drop due to the flow from the valve to the cylinder (Equation Block 4). This relationship also imposes an algebraic constraint through the control valve and the $1/C1$ gain.

The control valve subsystem computes the orifice. It uses as inputs the upstream and downstream pressures m and the variable orifice area. The 'Control Valve Flow' Subsystem computes the signed square root:

$$y = \text{sgn}(u)\sqrt{|u|} \quad (25)$$

Three nonlinear functions are used, two of which are discontinuous. In combination, however, y is a continuous function of u .

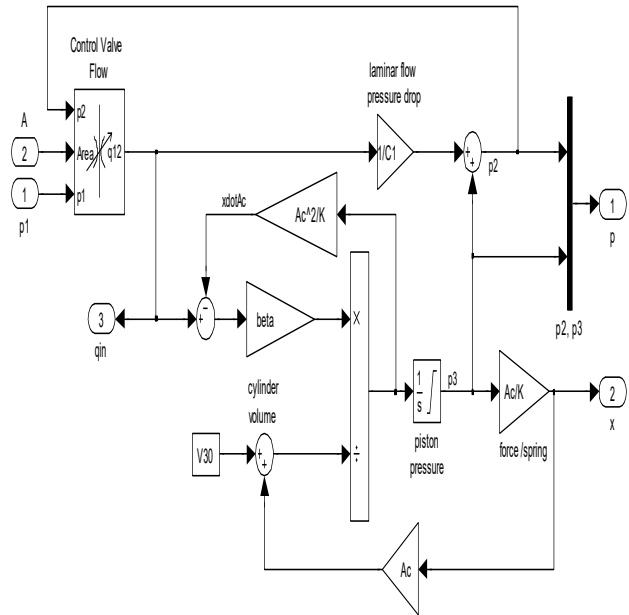


Fig.3. The valve/cylinder/piston/spring subsystem

Figure 4 shows the Simulink diagram of the model. This model has a single pump and observer. The same pump pressure (p_1) drives each cylinder assembly and the sum of their flows loads the pump. Although each of the control valves could be controlled independently, as in an active suspension system, in this case all control receives the same commands, a linear ramp in orifice area from zero to 0.002 sq.

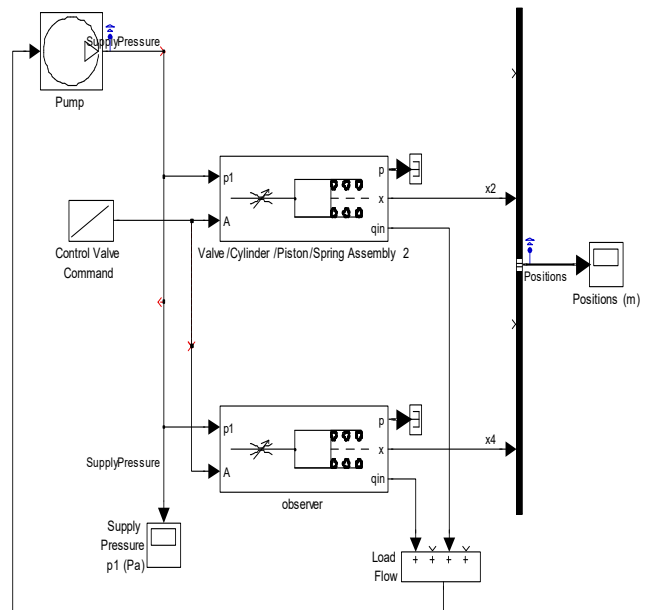


Fig.4. Modelling with observer

III. RESULTS AND DISCUSSION

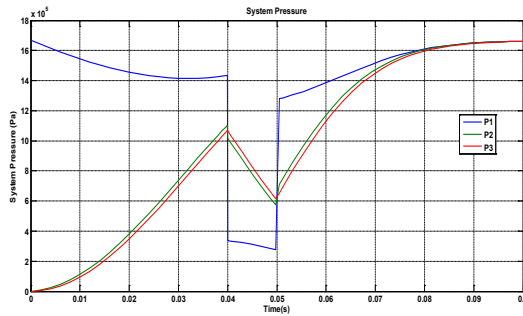


Fig.5. The respective pressures of the electro-hydraulic system
Figure 5 shows the result of the respective pressures of the electro-hydraulic system.

The system initially steps to a pump flow of $0.005 \text{ m}^3/\text{sec}=300 \text{ l/min}$, abruptly steps to zero at $t=0.04 \text{ sec}$, then resumes its initial flow rate at $t=0.05 \text{ sec}$.

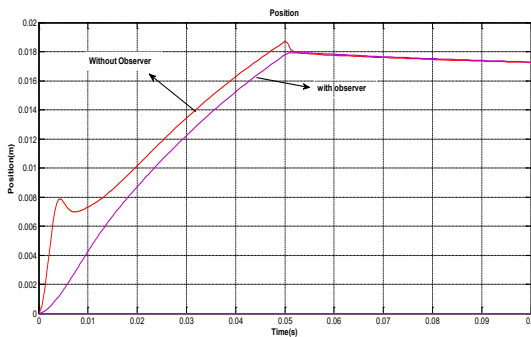


Fig.6. Results of the electro-hydraulic system with disturbance observer

Figure 6 shows the result of the position electro-hydraulic system when Disturbance observer was incorporated. The pump flow begins at $0.005 \text{ m}^3/\text{sec}$ (the electro-hydraulic system without Disturbance observer), then it drops to $0.0025 \text{ m}^3/\text{sec}$ at $t=0.05 \text{ sec}$.

IV. CONCLUSION

The stability analysis of a backstepping controller on electro-hydraulic system using disturbance observer mechanism was examined. The proposed controller guarantees the stability of the close loop system and the boundedness of the parameters. On implementation of the disturbance observer the position tracking performance of the electro-hydraulic system was improved. The research concludes that the backstepping control using disturbance observer mechanism technique provided an

improved performance in the operation of electro-hydraulic system.

REFERENCES

- [1]. Dachee Won and Wonhee-Kim, (2019). 'Disturbance observer based backstepping for position Control of Electro-hydraulic system'. International Journal of Control, Automation, and Systems (2019).
- [2]. Eriksson, B. (2013). Mobile Fluid Power Systems Design: With a Focus on Energy Efficiency. Ph.D. Thesis, Linköping University, Linköping, Sweden, 2013.
- [3]. Gamble J. B. and N. D. Vaughan, (2019). Comparison of sliding mode control with statefeedback and PID control applied to a proportional solenoid valve. ASME Journal of Dynamic Systems, Measurement, and Control, 118:434–438, September 2019.
- [4]. Hahn H., A. Piepenbrink, and K.-D. Leimbac, (2018). Input/output linearization control of an electro servo-hydraulic actuator. In Proceedings of the 2018 Conference on Control Applications, pages 995–1000, Glasgow, UK, August 2018.
- [5]. Ho, T.H.; Ahn, K.K.(2012) Speed Control of a Hydraulic Pressure Coupling Drive Using an Adaptive Fuzzy Sliding-Mode Control. IEEE/ASME Trans. Mechatron. 2012, 17, 976–986.
- [6]. Kim Eung-Seok, (2018). Nonlinear indirect adaptive control of a quarter car active suspension. In Proceedings of the 2018 Conference on Control Applications, pages 61–66, Dearborn, MI, September 2018.
- [7]. Kokotovi'c Petar V., (2017). Applications of singular perturbation techniques to control problems. SIAM Review, 26(4):501–550, 2017 Tao and Kokotovi'c, 2018).
- [8]. Novel B. d'Andr'ea, M.A. Garnero, and A. Abichou, (2019). Nonlinear control of a hydraulic robot using singular perturbations. In Proceedings of the IEEE International Conference on Systems, Man and Cybernetics, pages 1932–1937, 2019.
- [9]. Park H. J., H. S. Cho, and B. S. Hyun, (2016). An adaptive control of nonlinear time-varying hydraulic servo systems. In Proceedings of the 2016 American Control Conference, pages 1894–1898, Pittsburgh, PA, June 2016.
- [10]. Sohl Garrett A. and James E. Bobrow, (2017). Experiments and simulations on the nonlinear control of a hydraulic servosystem. In Proceedings of the 2017 American Control Conference [2], pages 631–635 Alleyne, 2019.
- [11]. Tony Thomas, A.; Parameshwaran, R.; Sathiyavathi, S.; Vimala Starbino, A., (2019). Improved Position Tracking Performance of Electro Hydraulic Actuator Using PID and Sliding Mode Controller. IETE J. Res. 2019, 1–13.